Journal of Applied Polymer Science

Influence of electrochemical copolymerization conditions of 3-methylthiophene and biphenyl on the morphology and nanomechanical properties of the films

Despina Triantou, Spyridon Soulis, Dimitris Perivoliotis, Costas Charitidis
National Technical University of Athens, School of Chemical Engineering, Laboratory Unit of Nanoengineering & Nanotechnology, Heroon Polytechniou 9, 157 73 Athens, Greece
Correspondence to: D. Triantou (E-mail: dstrian@gmail.com)

ABSTRACT: The aim of this work is to synthesize novel 3-methylthiophene (3MTh)/biphenyl (Biph) copolymer films by electropolymerization and study their mechanical properties through nanoindentation. The morphology, the chemical structure as well as the electrical conductivity of the copolymer films depended strongly on the electropolymerization conditions. It was found that the polymer deposition follow an instantaneous, two-dimensional nucleation and growth mechanism leading to homogenous films. The copolymer films had higher Young modulus and nanohardness than poly(3-methylthiophene) (3PMTh), indicating that the incorporation of Biph units within the P3MTh chain leads to a more densely packed structure and a more brittle polymer. © 2015 Wiley Periodicals, Inc. J. Appl. Polym. Sci. **2015**, *132*, 42575.

KEYWORDS: copolymers; conducting polymers; films; nanostructured polymers

Received 10 February 2015; accepted 4 June 2015
DOI: 10.1002/app.42575

INTRODUCTION

Electropolymerization is one of the best methods to deposit films of conducting polymers directly on a surface. In most cases, the film formed is actually grafted onto the surface, which is a prerequisite for good interphasial properties that are highly valued in every application (especially in electronics and photonics). Moreover, by controlling the operational parameters of the electropolymerization, it is possible to synthesize tailored polymers (i.e., with a combination of specific properties) that can fit certain applications.[1–4] A particularly interesting approximation to tailor the film properties is through copolymerization. It was proven that by using a combination of monomers, it is possible to synthesize copolymers possessing unique properties, even completely different than those of both the corresponding homopolymers.[4,5] In the works published up to now, the focus was on copolymerization of aromatic monomers (e.g., biphenyl, thiophene, pyrrole), either under potentiostatic or using dynamic (i.e., potential scanning) conditions. In all these cases, the films synthesized showed a wide variation in their morphology and properties.[4,6–10]

The films that were deposited through electropolymerization have been studied using plenty of methods, particularly spectroscopies, microscopies, and analytical techniques; however, their mechanical properties have only seldom been studied, even though their importance for the applications of these materials is widely recognized. The main reason for the absence of this kind of investigation is the difficulty to perform measurements into such thin films (with thickness a few micrometers at most). Rather recently, the development of nanoindentation opened new possibilities in this field. At first glance, this novel method seems an adaptation of the mechanical indentation test to nanoscale proportions: using a nanosized indenter tip (with known geometry), a force of several nanonewtons is applied and the indention into the sample is determined; however, this is rather an oversimplification, since nanoindentation has a substantially higher level of sophistication.[11] Additionally, this method involves sample penetration of a few nanometers and thus permits the measurement of thin samples like films. Using this method, the mechanical properties, hardness, and elastic modulus at the surface of the film and at depth of several nanometers can be estimated by analyzing the measured load–displacement curves. However, till today, there are only a few works about polymer films,[12–15] and even fewer about conducting polymers deposited by electropolymerization.

As already mentioned, electrochemical copolymerization has been confirmed as a versatile method to synthesize conducting films using combinations of aromatic monomers.[4] In previous work, we synthesized copolymer films based on 3-methylthiophene and biphenyl by electropolymerization; these films were applied as a hole transport layer in organic photovoltaic cells.[16] Even though

their properties (UV spectra, charge mobility) were suitable for such an application, the performance of the cells was low; this was attributed to the inhomogeneity of the deposited films. Therefore, in order to elucidate the mechanism of the film deposition, a thorough investigation on the effect of the electropolymerization conditions on the structure, the morphology, and the mechanical properties of the films (measured using nanoindentation) is necessary. The aim of this work is to begin this investigation.

EXPERIMENTAL

Materials

Biphenyl (Biph, Fluka) and 3-methylthiophene (3MTh, Fluka) were used as received. Tetrabutylammonium tetrafluoroborate ($TBABF_4$, Merck) was dried at 110°C up to constant weight. Acetonitrile (ACN, Merck, water content ~ 0.05%) was stored over molecular sieves (Fluka, 4 A, 8–12 mesh) prior to use.

Instrumentation

For the electropolymerization, a potentiostat Potentioscan Wenking POSS88 (Bank Elektronik) was used. The FTIR spectra of the polymers were recorded using a Perkin Elmer Spectrum GX spectrometer using KBr discs. The UV–vis spectra were recorded using a Varian Cary 300 spectrometer. The morphology of the films was examined by scanning electron microscopy (SEM) using a PHILIPS Quanta Inspect microscope (FEI Company) with W (tungsten) filament at 25 KV, equipped with an EDAX GENESIS (from AMETEX PROCESS & ANALYTICAL INSTRUMENTS). The DC electrical conductivity of the films at room temperature was determined with a two-probe technique,[17] using a multimeter.

Electropolymerization

The solution of the electropolymerization consists of the monomers dissolved into acetonitrile with $TBABF_4$ as supporting electrolyte. The monomers were used in concentration: [Biph]/[3MTh] = 0.05 M/0.05 M for copolymers and [3MTh] = 0.1 M for the poly(3-methylthiophene) homopolymer. The electrolyte concentration was [$TBABF_4$] = 0.1 M. All electropolymerizations took place at room temperature, in a one-compartment electrochemical cell of 60 mL volume using a system of three electrodes. The working electrode was either a Pt plate (4.5 cm^2) or an indium tin oxide (ITO)-covered glass (from PGO, Germany, active surface area: 1 cm^2). As counter electrode, a Pt plate was used (surface area: 9.0 cm^2) and as reference a calomel electrode (SCE) was placed into Luggin capillary. The solution was deoxygenated by bubbling nitrogen for 10 min before the beginning of the electropolymerization.

The polymer films were synthesized either under potentiostatic conditions (by applying a constant potential for a certain time) or by cyclic voltammetry (by scanning within a potential range with a defined scan rate). After the polymerization, the films were immersed in acetonitrile to remove $TBABF_4$ residues and the soluble oligomers and then were vacuum dried at 30°C up to constant weight. The thickness of the films was estimated from the charge during the electropolymerization or it was measured using a profilometer (reported values are the average of 10 measurements).

Nanoindentation

Nanoindentation testing was performed with a nanomechanical test apparatus, which allows the application of loads from 1 to 30,000 μN and records the displacement as a function of applied loads with a high load resolution (1 nN) and a high displacement resolution (0.04 nm). The nanomechanical test instrument employed in this study is equipped with a scanning probe microscope (SPM), in which a sharp probe tip moves in a raster scan pattern across a sample surface using a three-axis piezo positioner. In all nanoindentation tests, a total of 10 indents are averaged to determine nanomechanical values for statistical purposes, with a spacing of 50 μm, in a clean environment with 45% humidity and 23°C ambient temperature. In order to operate under closed loop load control (LC), feedback control option was used. The nanoindentation tests were conducted with a Berkovich (three-side pyramid) diamond indenter (average radius 100 nm) under a constant loading rate 40 μN/s and gradually increased to a predetermined value and held for 5 s before unloading gradually. Prior to indentation, the area function of the indenter tip was calibrated in a fused silica, a standard material for this purpose.[18] The applied load can be controlled at a constant value, whereas the penetration of the indenter tip into the sample surface is continuously recorded. This approach has been widely used both to study the time-dependent properties and to avoid nose effect of polymers.

Based on the elastic deformation theory, H and E values can be extracted from the experimental data of indenter load and displacement, i.e., Oliver–Pharr (O&P) method,[19] where derived expressions for calculating the elastic modulus from indentation experiments based on Sneddon's elastic contact theory:[20]

$$E_r = \frac{S\sqrt{\pi}}{2\beta\sqrt{A_c}} \tag{1}$$

where S is the unloading stiffness (initial slope of the unloading load–displacement curve at the maximum depth of penetration or peak load), A_c is the projected contact area between the tip and the substrate at peak load, and β is the constant that depends on the geometry of the indenter ($\beta = 1.167$ for Berkovich tip).[20,21] Conventional nanoindentation hardness refers to the mean contact pressure; this hardness, which is the contact hardness H_c, is actually dependent upon the geometry of the indenter (eq. 2):

$$H_c = \frac{F}{A_c} \tag{2}$$

Where

$$A(h_c) = 24,5h_c^2 + a_1 h_c + a_{1/2} h_c^{1/2} + \ldots + a_{1/16} h_c^{1/16} \tag{3}$$

and

$$h_c = h_m - \varepsilon \frac{P_m}{S_m} \tag{4}$$

where h_m is the total penetration depth of the indenter at peak load, P_m is the peak load at the indenter displacement depth h_m, and ε is an indenter geometry constant, equal to 0.75 for Berkovich indenter.[20] For polymer films, Poisson's ratio v is taken as 0.40. The elastic modules and Poisson's ratio for the indenter (diamond) are 1140 GPa and 0.07, respectively.

Table I. Experimental Parameters and Characteristics (Thickness, Color) of Synthesized Films

	Experimental parameters					Characteristics of films synthesized	
	Cyclic Voltammetry			Potentiostatic			
Code of films	Scan range (V vs SCE)	Scans	Scan rate (mV/s)	Appl. Potential (V)	Time (min)	Thickness (μm)	Color
$(3MTh\text{-}Biph)_{1.55/30}$				1.55	30	8.00[a]	Dark blue
$(3MTh\text{-}Biph)_{1.55/5}$				1.55	5	0.90[a]	Blue
$(3MTh\text{-}Biph)_{1.55/2}$				1.55	2	0.35[a]	Blue
$(3MTh\text{-}Biph)_{1.57/2}$				1.57	2	0.45[a]	Blue
P3MTh	$0 \rightarrow +2.0 \rightarrow 0$	6	20			2.5 ± 0.5[b]	Blue
$(3MTh\text{-}Biph)_1$	$+1 \rightarrow +2.0 \rightarrow +1$	1	10			2.0 ± 0.4[b]	Dark blue
$(3MTh\text{-}Biph)_2$	$+1 \rightarrow +2.0 \rightarrow +1$	5	100			1.4 ± 0.2[b]	Blue
$(3MTh\text{-}Biph)_3$	$0 \rightarrow +2.0 \rightarrow 0$	3	20			1.7 ± 0.4[b]	Red

[a] Thickness was estimated form the charge during the electropolymerization.
[b] Thickness was measured by profilometer.

Hardness and Young's modulus values were extracted from the experimental data (load–unload curves) using the Oliver and Pharr (O&P) method.

RESULTS AND DISCUSSION

Synthesis of the Polymer Films by Electropolymerization

Under potentiostatic conditions, electropolymerization can be achieved when the applied voltage is above the oxidation potential (E_{ox}) of the monomer (or, in the current case, of the combination of monomers). The experimental procedure for determining E_{ox} has been described in our previous work.[6] For the Biph–3MTh monomer system, E_{ox} was estimated as 1.55 V (vs SCE). In order to investigate the effect of the experimental conditions on the properties of the films, electropolymerization experiments were performed using different potential applied for different time (duration). Table I presents the experimental parameters and the characteristics (thickness and color) of the corresponding synthesized copolymer films. Figure 1 presents the current–time curve during the synthesis of the copolymers $(3MPTh\text{–}Biph)_{1.55/30}$ and $(3MPTh\text{–}Biph)_{1.57/2}$.

Copolymer films were also synthesized using cyclic voltammetry, under different potential ranges and scan rates. Specifically, either a wide potential range (from 0 V up to +2 V) or a narrow one (from +1 V up to +2 V) was used. The number of scans and the scan rate were selected in order to synthesize homogeneous films having an approximate thickness of 2.0 μm. For comparison, 3PMTh homopolymer film was also synthesized by CV using the wide potential range (from 0 V to +2 V). Figure 2 presents the volammograms during the synthesis of the 3PMTh homopolymer and of the copolymer films onto ITO

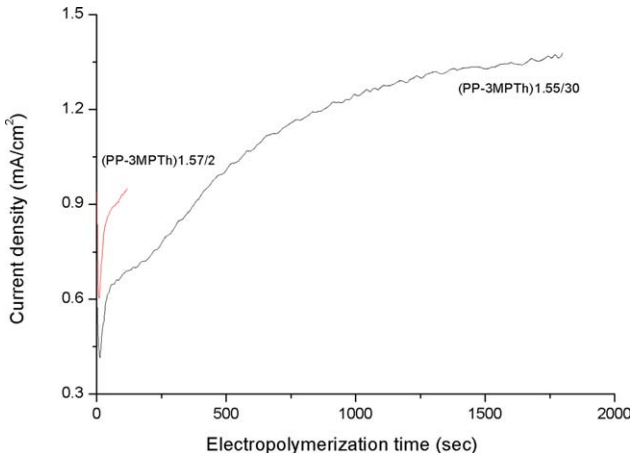

Figure 1. Current versus time (i)–(t) curves during the electropolymerization of 3-methylthiophene with biphenyl under different applied potentials (for the codes, see Table I). [Color figure can be viewed in the online issue, which is available at wileyonlinelibrary.com.]

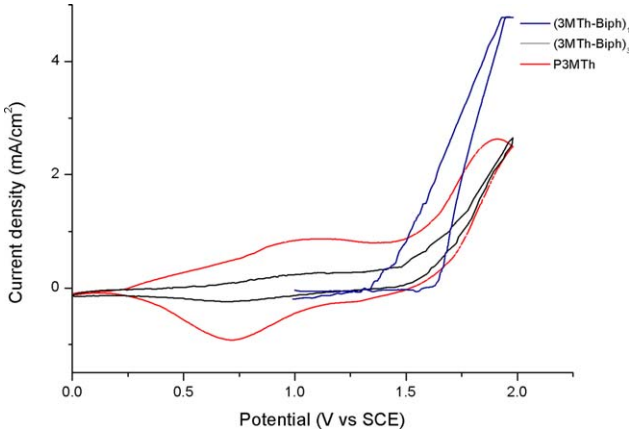

Figure 2. Cyclic voltammograms during the electropolymerization of P3MTh and 3MTh–Biph monomers system onto ITO electrodes. In all cases, the last scan is presented, i.e., the sixth scan for P3MTh, first scan for $(3MTh\text{–}Biph)_1$, and third scan for $(3MTh\text{-}Biph)_2$ (for the codes, see Table I). [Color figure can be viewed in the online issue, which is available at wileyonlinelibrary.com.]

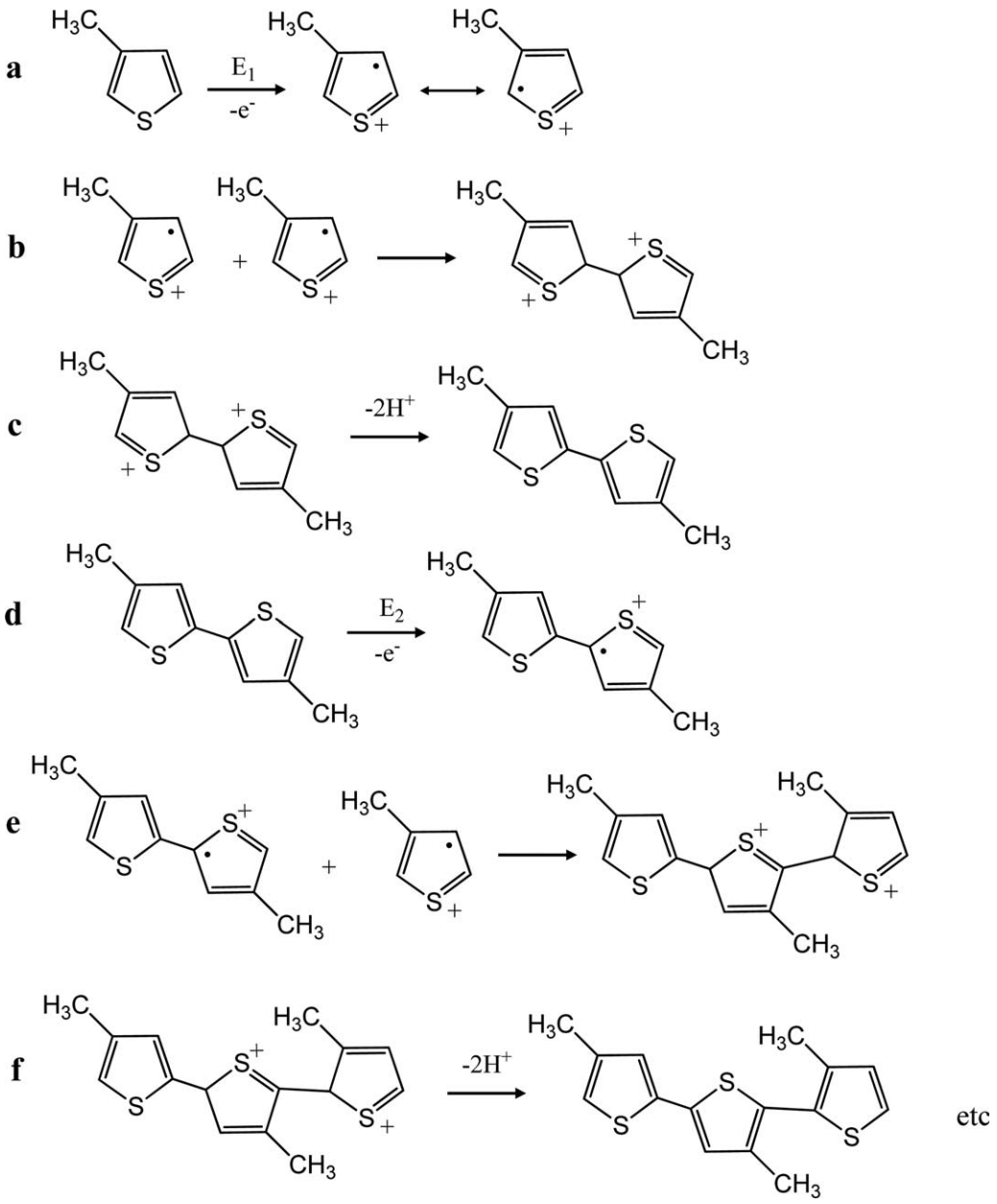

Scheme 1. Electropolymerization mechanism of 3-methylthiophene.

electrodes. During the deposition of the 3PMTh, at the first scan, it can be seen that the oxidation of the monomer begins at around 1.2 V. In the subsequent scans, the voltammogram exhibits a couple of redox peaks (as it can be seen during the sixth scan): one broad oxidation peak centered at about 1.0 V (starting from about 0.8 V) due to the oxidation (or doping) of the already deposited polymer and one reduction peak centered at around 0.7 V during the dedoping of the polymer. The broad oxidation peak can be attributed to the overlapping of the peaks due to the oxidation of the monomer and the doping of the polymer.

Similar to 3PMTh, copolymer $(3MTh–Biph)_3$ exhibits a redox couple due to oxidation/reduction of the polymer (third scan). More specifically, it has a broad oxidation peak, centered at about 1.1 V (starting from about 0.8 V) and a reduction peak at about 0.75 V, due to the doping and dedoping of the copolymer, respectively. The copolymer changes its color from blue in the forward scan direction (from 0 to +2 V) to red in the reverse scan direction (from 2 to 0 V). In the case of $(3MTh–Biph)_1$, the oxidation begins immediately at about 1.2 V, but no peak can be distinguished (first scan). At the same time, not any negative (cathodic) current is observed, indicating the absence of any reduction phenomena (i.e., dedoping). Consequently, the $(3MTh–Biph)_1$ film is in the oxidized state (having dark blue color), opposite to $(3MTh–Biph)_3$ which is at least partially reduced and has red color (see also Table I).

In order to estimate the oxidative state of the polymer films synthesized (i.e., if they were oxidized or reduced, either totally

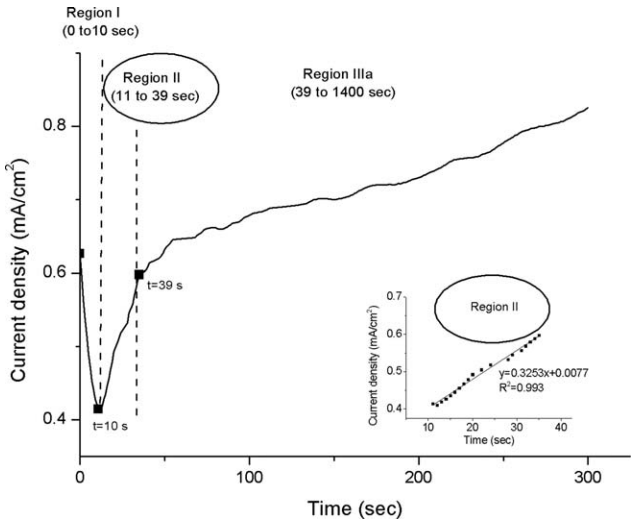

Figure 3. Current versus electropolymerization time from 0 to 300 s for copolymer $(3MTh–Biph)_{1.55/30}$, (for the code, see Table I). The Region III_a continues up to 1400 s and then the Region III_b appeared up to 1800 s.

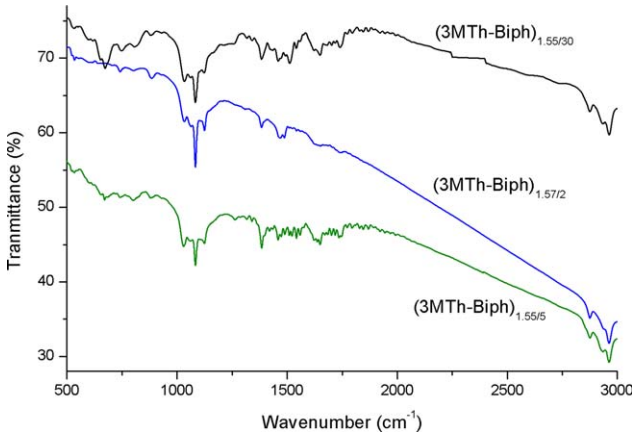

Figure 4. FTIR spectra of the copolymer film synthesized by potentiostatic electropolymerization (for the codes, see Table I). [Color figure can be viewed in the online issue, which is available at wileyonlinelibrary.com.]

or partially), the ratio of the oxidation to reduction charge (Q_{ox}/Q_{red}) was calculated for each scan. The P3MTh film has a ratio of 2.8, indicating that it is partially oxidized (blue color). Similarly, copolymer $(3MTh–Biph)_3$ has a ratio of 6.5 and is also partially oxidized (red color), whereas $(3MTh–Biph)_1$ and $(3MTh–Biph)_2$ have only (or mainly) oxidation charge ($Q_{ox}/Q_{red} = 14$) and are fully oxidized (with dark blue and blue color, respectively).

Electropolymerization Mechanism

The electropolymerization mechanism of 3MTh is presented in Scheme 1. The first step is the oxidation of the monomer (Scheme 1a) and the formation of the radical cation. Then, two radical cations are coupled and the dihydrodimer dication (Scheme 1b) is formed. The latter, after losing two protons and rearomatizing, is converted to the dimer (Scheme 1c). The dimer is oxidized (more easily than the monomer) and following the same route (Scheme 1d–f), the trimer is formed. Following these reactions, the polymer chain keeps growing on.

From the current–time (i)–(t) curves of the potentiostatic electropolymerization, the mechanism of the film deposition could be derived. It is well known that the basic reaction steps take place within the first 2 min. In Figure 3, the initial part of the (i)–(t) curve of the copolymer $(3MPTh–Biph)_{1.55/30}$ is shown. Thus, according to the mechanism of the deposition, the (i)–(t) curves can be analyzed in regions where specific steps of the film deposition take place.[6,7,22] Namely, there are the following regions:

- *Region I:* Charging of the interface between the working electrode and the electrolytic solution.
- *Region II:* Nucleation and growth of the polymer film. Following the progress of the reaction, oligomers are formed containing 2–5 aromatic rings which become increasingly less soluble until they become large enough (i.e., polymer) and are deposited onto the working electrode as the nuclei of the film.
- *Region III:* The growth of the already mentioned nuclei continues (Region III_a), but with smaller rate than that of Region II. After a certain time, the growth rate is stabilized and the film is formed, resulting to a current plateau (Region III_b).
- *Region IV:* The film growth rate decreases, due to the overlapping of the growing nuclei and due to the diffusion of the radical cations form the interphase to the electrolytic solution (i.e., they do not any longer take part in the film growth). Moreover, it is possible to observe an almost constant current, indicating that the film growth follows a steady rate. The time where the current reaches constant value depends on the applied potential and as a general rule, usually it decreases with increasing applied potential.

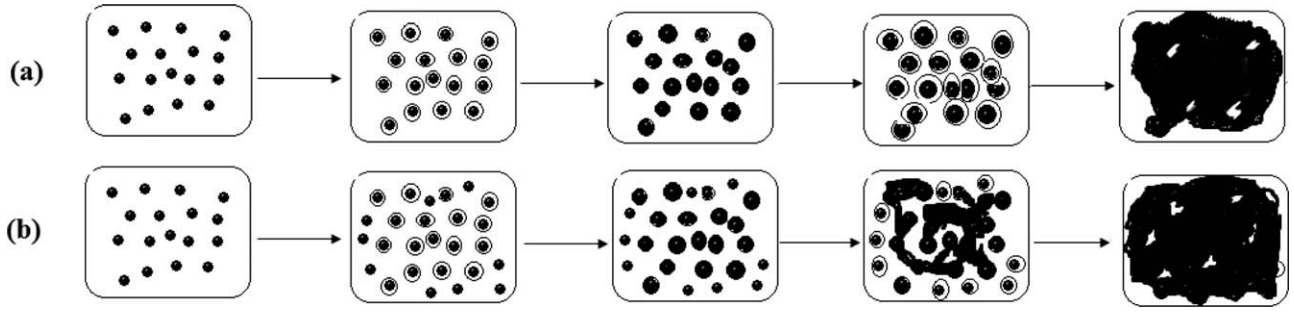

Scheme 2. (a) Instantaneous and (b) progressive nucleation.

Table II. Description of FTIR Bands of the Copolymers

Characteristic bonds	Wavenumber (cm^{-1})
$>CH_2$: aliphatic (cyclic and linear) parts	2960, 2920, 2870
C=O: bending vibrations	1740-1710
C=C: stretching vibrations of the phenylene ring due to the biphenyl units	1600
Quinoid structure	1570
Benzenoid structure	1480
C—C: stretching vibrations of aromatic ring	1400
	1375
Methyl deformation of 3MTh units	1312
C—H "in-plane" vibrations	1240
	1165
	980
	943
CH_3: of 3MTh units	890
C—H: short terminal phenylene rings	740
C—S—C ring deformations due to 3MTh units	680
C—S bending vibrations due to 3MTh units	600

The nucleation and growth mechanism (NGM) can be determined from the analysis of Region II. According to the literature,[6,23,24] there are two types of nucleation: instantaneous (I) and progressive (P). In instantaneous nucleation, the number of nuclei is constant, and they grow on their former positions on the bare substrate surface without the formation of new nuclei. Hence the radii of nuclei are larger and the surface morphology is rougher (Scheme 2a). In progressive nucleation, the nuclei grow not only on their former positions, but also on new nuclei which form smaller particles and the surface morphology is more flat (Scheme 2b). Concerning the growth of the film, this could be in one (1D), two (2D), or three (3D) dimensions. In the 3D, the growth rates of nuclei in the parallel and perpendicular to the electrode surface directions are essentially equal or comparable. Similarly, in the 2D growth, the nuclei grow more quickly in the parallel than the perpendicular direction until they meet and overlap. In addition to the above, all the types of NGM can be controlled either by diffusion or charge transfer. The type of NGM can be determined from the plot of (i) versus t^x, where x is $-(1/2)$, (1/2), 1, 2, 3, and (3/2), finding which power law gives linear relationship between (i) and t^x.[6,7] NGM can only be determined when Region II is well defined.

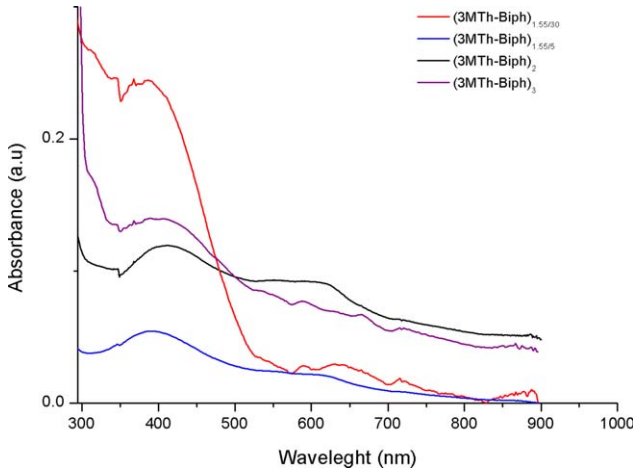

Figure 5. UV–vis spectra of the copolymer films in DMF (for the codes, see Table I). [Color figure can be viewed in the online issue, which is available at wileyonlinelibrary.com.]

It has already been proven that for polyphenylenes $x = 1$ and that for 3PMTh $x = 0.5$, independent of the applied potential.[6,7] This means that the NGM is instantaneous, two-dimensional nucleation (IN2D) in both cases, controlled by charge transfer in the former case and diffusion in the latter. The copolymers also have $x = 1$ in the whole range of applied potentials which was investigated. This means that the growth takes place in two dimensions (2D), as layer by layer.[22] The properties of the deposited film depend on the nucleation mechanism. The growth mechanism is very important for the quality of the films, since 2D growth leads to compact films whereas 3D growth leads to loose, powder like-films. For example, compact films are formed by 2D nucleation, by instantaneous nucleation with 3D growth rough grains are formed, whereas progressive 3D grow leads to more homogenous grains.[22] In our case, the films grow 2D that means that the deposited films are expected to be compact.

Structural Analysis of the Copolymers

In Figure 4, the FTIR spectra of the copolymers deposited on Pt electrodes are presented. The various bands of the copolymers are presented in Table II with respect to the assigned chemical structures.[4,5,16]

In Figure 5, the UV spectra of the copolymers in dimethylformamide are shown. The copolymers exhibit two absorption bands at 390 and 600 nm. Comparing the spectra of the copolymers that were synthesized using the same potential but different electropolymerization duration, it can be observed that the peak absorbance increases with respect to the duration, leading to a more narrow and sharp peak at 388 nm. Copolymer (PP–3MPTh)$_2$ exhibits two bands at 410 and at 615 nm, whereas (PP–3MPTh)$_3$ has one at 407 nm and also an absorption shoulder at 590 nm. The main absorption that is attributed to the copolymer (at 410 nm) shifts to higher wavelengths when the polymer is more highly doped, i.e., for (PP–3MPTh)$_2$.

Table III. Electrical Conductivity of the Polymers Films on Pt Electrodes

Code of the polymer	Electrical conductivity (S/cm^2)
$(P3MTh\text{-}Biph)_{1.55/30}$	4.0×10^{-1}
$(P3MTh\text{-}Biph)_{1.55/5}$	9.0×10^{-1}
$(P3MTh\text{-}Biph)_{1.55/2}$	8.0×10^{-1}
$(P3PTh\text{-}Biph)_{1.57/2}$	8.7×10^{-3}
$(3MTh\text{-}Biph)_1$	7.0×10^{-1}
$(3MTh\text{-}Biph)_2$	4.2×10^{-2}
$(3MTh\text{-}Biph)_3$	5.0×10^{-3}

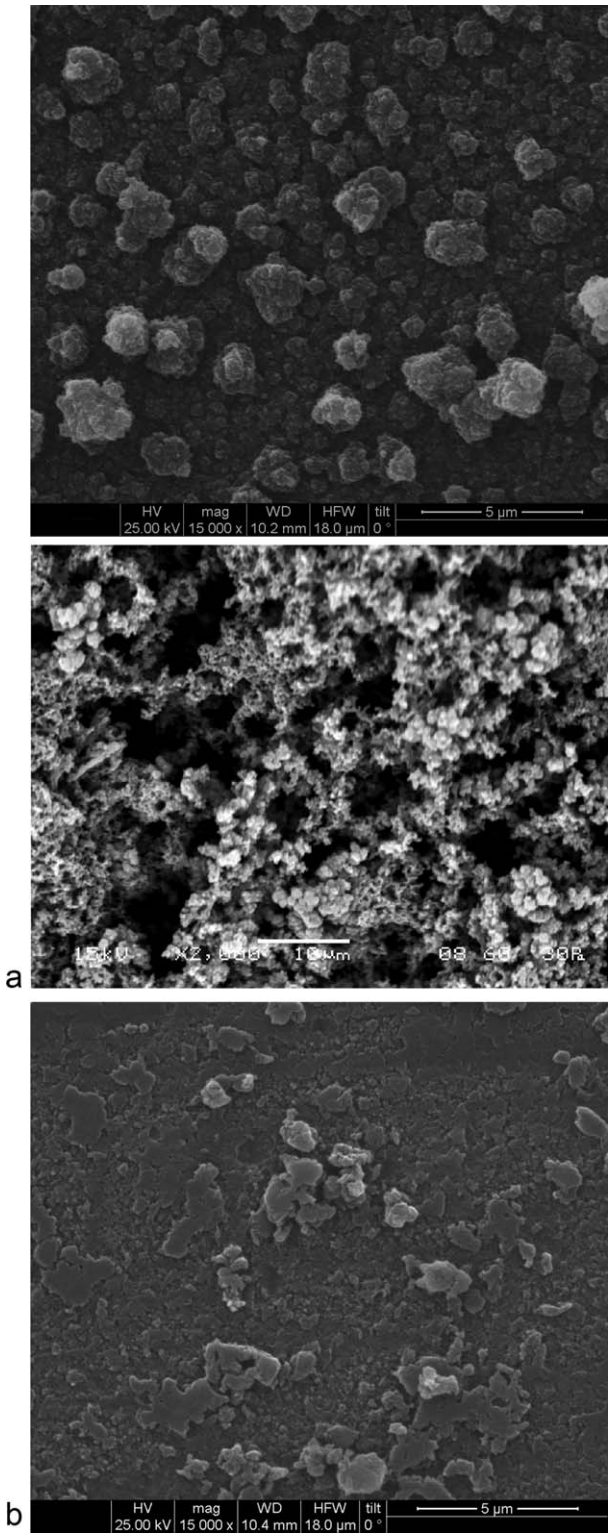

Figure 6. SEM photographs of polymer films synthesized by potentiostatic electropolymerization on Pt electrode: (a) $(3MTh–Biph)_{1.55/30}$ and (b) $(3MTh–Biph)_{1.55/5}$ (for the codes, see Table I).

Electrical Conductivity

The electrical conductivity of the films synthesized on Pt electrode is presented in Table III. Comparing the films deposited under the same applied potential, the electrical conductivity decreases by increasing the electropolymerization duration. For 1.55 V, the film deposited under 30 min has the lower conductivity; this is because it is thick and less uniform (see the section titled "Morphology and Elemental Analysis of the Copolymers") than the thin ones (synthesized for 5 or 2 min). By increasing the applied potential, the conductivity also decreases. In the case of the films synthesized by cyclic voltammetry, both the scan rate and the potential range affect strongly the conductivity. Namely, the conductivity decreases when the scan rate increases (cf. copolymers 1 and 2) and when the wide potential range is used (cf. copolymers 1 and 3). In the latter case, this is due to the reduction of the copolymers that take place during the scanning. The electrical conductivity of the copolymers can be also correlated with the morphology of the films (see the section titled "Morphology and Elemental Analysis of the Copolymers").

Morphology and Elemental Analysis of the Copolymers

Before performing a nanoindentation measurement, it is important that the morphology of the films be known; this can be determined using some kind of microscopic method. Here, the morphology of the films deposited onto ITO was studied by scanning electron microscopy (SEM). In Figure 6, the SEM photographs of the copolymers films synthesized by potentiostatic electropolymerization are presented. The copolymer $(3MTh–Biph)_{1.55/30}$ [Figure 6(a)] has a sponge-like morphology with 1.2–2.0 μm diameter aggregates. On the other hand, $(3MTh–Biph)_{1.55/5}$ [Figure 6(b)] has a granular morphology with aggregates of 2 μm. The effect of the polymerization duration on the films morphology is obvious: $(3MTh–Biph)_{1.55/5}$ is more uniform than the film synthesized for higher electropolymerization duration and this affects also the conductivity; namely, the thin film has higher conductivity than the thicker one.

In Figure 7, the SEM photographs of the films synthesized by cyclic voltammetry are presented. The homopolymer P3MTh [Figure 7(a)] is composed of a continuous thin layer with protruding grains having a size of few micrometers. These grains appear to be composed of stacked layers (lamellae). Similar structure has the copolymer $(3MTh–Biph)_3$ [Figure 7(d)], but the grains are generally larger and more extended; additionally, some grain aggregates appear, having a size of few micrometers. Since the two films were synthesized using the same potential range and scanning rate, the differences in the morphology should be attributed to the effect of the comonomer. It seems that the presence of biphenyl affords more compact films. This can be supported from previous works about copolymers of biphenyl with thiophene[6] or biphenyl with pyrrole,[7] where the copolymers were generally more compact compared to the thiophene or pyrrole homopolymers. Copolymer $(3MTh–Biph)_1$ [Figure 7(b)] has completely different morphology: again, the main feature of the film are the thin flat lamellae, but this time they appear thinner and more porous; however, it also has a uniform morphology. Comparing the film $(3MTh–Biph)_1$ with $(3MTh–Biph)_2$ [Figure 7(b,c)], the effect of the scan rate on the morphology can be observed. The low scan rate leads to a more uniform film compared to the one deposited with a higher scan rate, which has big aggregates that disturb the

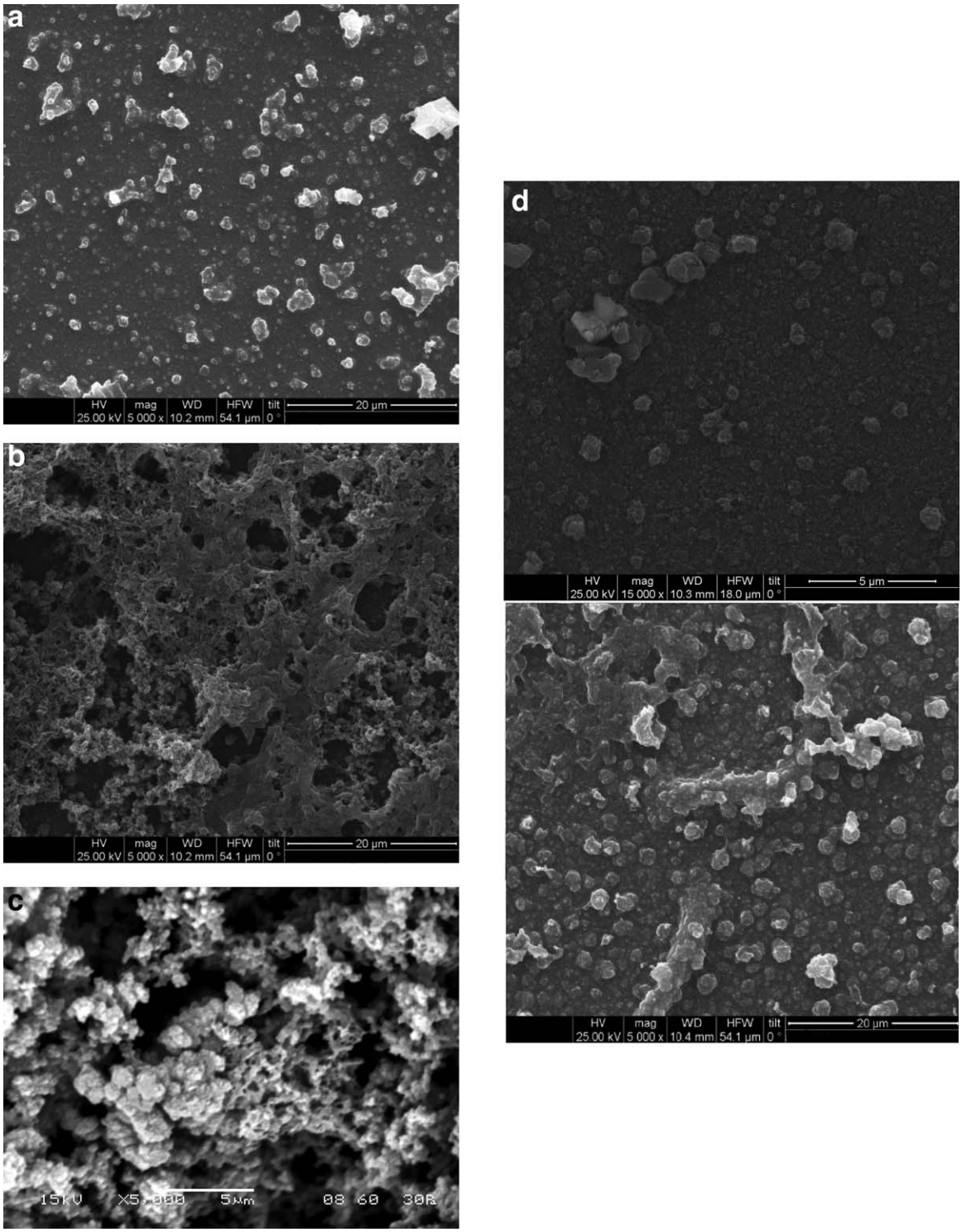

Figure 7. SEM photographs of polymer films synthesized by cyclic voltammetry on ITO electrode: (a) (P3MTh), (b) $(3MTh–Biph)_1$, (c) $(3MTh–Biph)_2$, and (d) $(3MTh\text{-}Biph)_3$ (for the codes, see Table I).

uniformity. Similarly, comparing the film $(3MTh–Biph)_1$ with $(3MTh–Biph)_3$ [Figure 7(b,d)], the effect of the potential range on the morphology can be observed; they have a totally different morphology. The main reason for this is likely the difference in the doping level: $(3MTh–Biph)_1$ is fully doped, containing a large amount of positive charges on the chains. Consequently, a similarly large amount of BF_4^- counterions should be present. These ions disturb the ordering of the molecules inside the lamellae and the stacking of them into dense grains. On the other hand, $(3MTh–Biph)_3$ is partially reduced containing much less counter ion (see also Table III for the values of the conductivity).

Table IV. Ratio of the Biphenyl to 3-methythiophene Structural Units

Code of the polymer	Ratio of the structural units
	Biph/3MTh
$(P3MTh\text{–}Biph)_{1.55/30}$	1/1.30
$(P3MTh\text{–}Biph)_{1.55/5}$	1/0.55
$(P3MTh\text{–}Biph)_{1.55/2}$	1/0.44
$(P3PTh\text{–}Biph)_{1.57/2}$	1/0.73
$(3MTh\text{–}Biph)_1$	1/1.15
$(3MTh\text{–}Biph)_2$	1/1.66
$(3MTh\text{–}Biph)_3$	1/1.00

It is clear that the copolymers are composed of (more or less) planar lamellae stacked one over the other. From the mechanism of the potentiostatic electropolymerization, it was found that the deposition of the copolymer films follows an instantaneous, 2D NGM. As already mentioned, this kind of mechanism affords compact films consisting of flat crystallites. The SEM photos indicate that the same nucleation and growth mechanism takes place during electropolymerization under potential scanning (i.e., cyclic voltammetry) conditions. The initial lamellae seem to have dimensions of a few micrometers, but they tend to aggregate forming the continuous layers seen in the background. However, it is also evident that the growth of the copolymer film is not uniform; in some places, the stacking of the lamellae has led to the formation of grains that protrude from the more homogenous film in the background.

For the copolymers, the ratio of structural units derived from biphenyl per that derived from 3-methylthiophene was calculated according to the literature.[6,7] The values are presented in Table IV. The morphology of the copolymers can also be correlated with the ratio of structural units. Comparing $(3MTh\text{–}Biph)_{1.55/30}$ with $(3MTh\text{–}Biph)_{1.55/5}$, the former contains more 3MTh than the latter; this may explain why the latter is more uniform. Similar conclusions can be derived when comparing the films synthesized by cyclic voltammetry: film $(3MTh\text{–}Biph)_1$ contains more biphenyl units and is more uniform that $(3MTh\text{–}Biph)_2$ and, at the same time, film $(3MTh\text{–}Biph)_3$ contains equal structural units of Biph and 3MTh and is more uniform than $(3MTh\text{–}Biph)_1$.

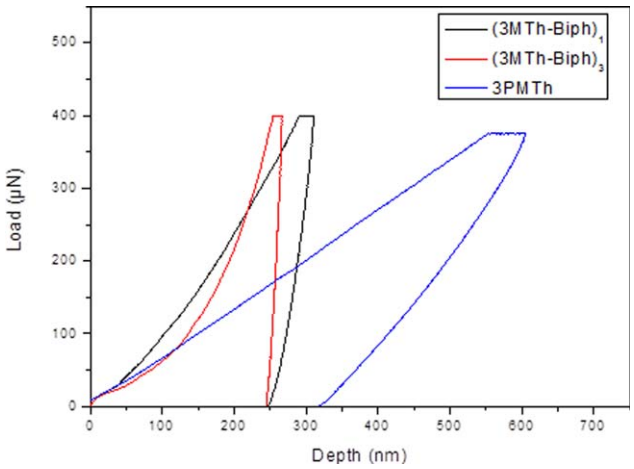

Figure 8. Load–depth curves of the three different polymer films onto ITO substrates obtained by nanoindentation under maximum load (400 μN). [Color figure can be viewed in the online issue, which is available at wileyonlinelibrary.com.]

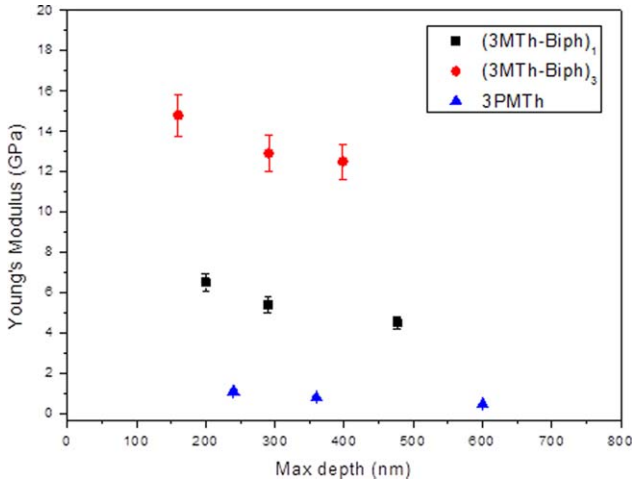

Figure 9. Young's modulus profiling of $(3MTh\text{–}Biph)_1$, $(3MTh\text{–}Biph)_3$, and 3PMTh films. [Color figure can be viewed in the online issue, which is available at wileyonlinelibrary.com.]

Nanomechanical Properties

Nanoindentation is the most commonly used technique to obtain local mechanical properties of small volume materials. Nanoindentation results are presented in Figures 8–10. Figure 8 compares the load–depth curves of the three different polymer films onto ITO substrates obtained by nanoindentation under the maximum load (400 μN). The film of 3PMTh displays different nanomechanical behavior than the copolymer films, which have similar (but not identical) behavior. Specifically, the maximum penetration depth is higher for 3PMTh (about 600 nm) compared with the copolymers (250–300 nm), indicating that the former material is more ductile than the latter.

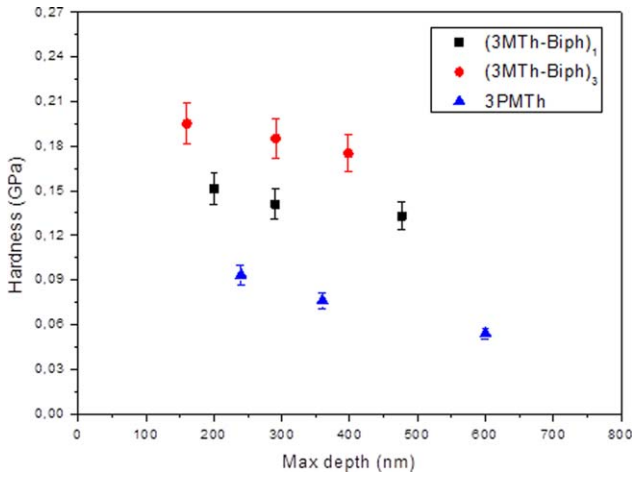

Figure 10. Hardness profiling of $(3MTh\text{-}Biph)_1$, $(3MTh\text{-}Biph)_3$, and 3PMTh films. [Color figure can be viewed in the online issue, which is available at wileyonlinelibrary.com.]

Figures 9 and 10 illustrate the calculated values of the Young modulus (E, in GPa) and the indentation nanohardness (H, in GPa) of the three different materials as a function of penetration depth (h_{max}, nm). A general trend observed in both E and H is that they decrease by increasing the indentation load. This observation could be attributed to indentation size effect (*ISE*).[25,26] At present, this phenomenon cannot be exhaustively explained, but it is likely due to a combination of factors, e.g., surface nano-roughness, adhesive forces between the tip and the sample, imperfection in tip geometry, formation of an intrinsic harder outer skin in the outermost surface layer of the specimen, etc.[25,27] Till today, there are not many works on the nanomechanical properties of conducting polymers; in the literature, only P3HT has already been studied and the E and H values that have been reported are of 1.4 and 0.08 GPa, respectively.[28] These values are very close to those measured in the case of the P3MTh film, where the average of the Young modulus and of the hardness was about 1.0 and about 0.06 GPa, respectively.

Concerning the copolymer films, both of them have higher values of measured nanomechanical properties than those of the P3MTh homopolymer film. This can be attributed mainly to the incorporation of biphenyl unit into the structure. Given that biphenyl is not substituted in any position, it can be expected that the incorporation of such a unit will increase the rigidity of the polymer backbone; however, at the same time, the loss of chain regularity may also lead to subsequent decrease of the polymer crystallinity. It seems that the increase of the rigidity is high enough to compensate for any loss of crystallinity. Since the copolymer film had higher properties than those of homopolymer (measured using similar methodology), the use of the copolymer film into a device will act with a double role, i.e., apart from its electronic function, it will also act as a load-bearing component.

Comparing the nanomechanical properties of the two 3MTh–Biph copolymer films, it is clearly observed that both elastic modulus and hardness values decrease with increasing degree of doping. This could be attributed to the presence of the anions BF_4^- incorporated into the doped polymer film in order to maintain electric neutrality. The role of these anions is not limited to the stabilization of the opposite charge but they also are likely to play a key role in the formation of the structure of the polymer chains affecting on both the physical and mechanical properties of the whole polymer film.[28–31]

CONCLUSIONS

Novel electrically conducting copolymer films were synthesized by electropolymerization based on the combination of biphenyl with 3-methylthiophene and their nanomechanical properties were investigated. The films were deposited using either potentiostatic or cyclic voltammetric conditions. From the potentiostatic electropolymerization, the nucleation and growth mechanism (NGM) was determined as instantaneous, two-dimensional controlled by charge transfer, affording homogenous films; the same mechanism appears to describe the film growth during cyclic voltammetry. The effects of the electropolymerization conditions on the morphology, chemical structure, and electrical conductivity of the copolymer films were investigated. More homogenous films with higher conductivity were produced when using applied potential near the onset of the electropolymerization and lower duration (for potentiostatic conditions) or smaller scanning rate and a narrow scanning range (avoiding reduction, in cyclic voltammetry). The copolymer films had higher Young modulus and nanohardness than poly(3-methylthiophene), indicating that the incorporation of biphenyl leads to a more densely packed structure and a more brittle polymer. The thinner films deposited at low number of scans were better adhered onto the substrate and had higher wear resistance compared to the thick films, especially at low indentation depths.

REFERENCES

1. Bidan, G. In Electropolymerization: Concepts, Materials and Applications; Serge Cosnier; Arkady Karyakin, Eds.; Wiley: New York, **2010**; p 1.
2. Zotti, Z. In Handbook of Conductive Molecules and Polymers; Nalwa, H. S., Ed.; Wiley: New York, **1997**; Vol. *2*, p 137.
3. Sezai, Sarac, A. In Encyclopedia of Polymer Science and Technology; Wiley: New York, **2006**, Vol. *6*, 1.
4. Simitzis., J.; Soulis, S.; Triantou, D. In Conducting Polymers: Synthesis, Properties and Applications; Pimentel, A., Ed.; Nova Science Publishers: New York, **2013**, 27.
5. Simitzis, J.; Triantou, D.; Soulis, S. *J. Appl. Pol. Sci.* **2008**, *110*, 356.
6. Simitzis, J.; Triantou, D.; Soulis, S. *J. Appl. Pol. Sci.* **2010**, *118*, 1494.
7. Simitzis, J.; Soulis, S.; Triantou, D. *J. Appl. Pol. Sci.* **2012**, *125*, 1928.
8. Dang, X. D.; Intelmann, C. M.; Rammelt, U.; Plieth, W. *J. Sol. St. Electrochem.* **2004**, *8*, 727.
9. Gumbs, R. W. In Handbook of Organic Conductive Molecules and Polymers; Nalwa, H. S., Ed.; Wiley: Chichester, **1997**; p 469.
10. Turac, E.; Sahmetlioglu, E.; Toppare, L. *J. Macromol. Sci. Part A* **2014**, *51*, 210.
11. Fischer-Cripps, A. C. Nanoindentation, 3rd ed. Springer: New York, **2011**.
12. VanLandingham, M. R.; Villarrubia, J. S.; Guthrie, W. F.; Meyers, G. F. Nanoindentation of Polymers: An Overview; Tsukruk, V. V.; Spencer, N. D., Eds.; Macromol Symposia, Wiley: New York, **2001**, 15.
13. Geng, K.; Yang, F.; Druffel, T.; Grulke, E. A. *Polymer* **2005**, *46*, 11768.
14. Fanga, T. E.; Chang, W. J. *Microelectronics J.* **2004**, *35*, 595.
15. Charitidis, C. *Ind. Eng. Chem. Res.* **2011**, *50*, 565.
16. Triantou, D.; Soulis, S.; Koureli, S.; De Sio, A.; Von Hauff, E. *J. Appl. Polym. Sci.* **2013**, *127*, 585.
17. Blythe, A. R. Electrical Properties of Polymers; Cambridge University Press: Cambridge, **1979**.
18. Charitidis, C.; Dragatogiannis, D.; Koumoulos, E.; Kartsonakis, I. *Mat. Sci. Eng. Part A* **2012**, *540*, 226.

19. Oliver, W. C.; Pharr, G. M. *J. Mat. Res.* **1992**, *7*, 1564.
20. Sneddon, I. N. Mathem. Proc. Cambridge Philosophical Soc. **1948**, *44*, 492.
21. King, R. B. *Int. J. Sol. Stru.* **1987**, *23*, 1657.
22. Vignali, M.; Edwards, R. A. H.; Serantoni, M.; Cunnane, V. J. *J. Electroanal. Chem.* **2006** *591*, 59.
23. Hwang, B. J.; Santhanam, R.; Lin, Y. L. *J. Electrochem. Soc.* **2000**, *147*, 2252.
24. Hwang, B. J.; Santhanam, R.; Wu, C. R.; Tsai, Y. W. *Electroanalysis* **2001**, *13*, 37.
25. Uzun, O.; Basman, N.; Alkan, C.; Kolemen, U.; Yilmaz, F. *Polym. Bull.* **2011**, *66*, 549.
26. Charitidis, C. A.; Koumoulos, E. P.; Nikolakis, V.; Dragatogiannis, D. A. *Thin Solid Films* **2012**, *526*, 168.
27. Biran, C.; Toppare, L.; Tinçer, T.; Yagci, Y.; Harabagiu, V. *Chem. Eng. Commun.* **2003**, *190*, 823.
28. Worfolk, B. J.; Rider, D. A.; Elias, A. L.; Thomas, M.; Harris, K. D.; Buriak, J. M. *Adv. Funct. Mater.* **2011**, *21*, 1816.
29. Tamm, J.; Aluma, A.; Hallik, A.; Silk, T.; Sammelselg, V. *J. Electroanal. Chem.* **1996**, *414*, 149.
30. Lee, H.; Yang, H.; Kwak, J. *J. Phys. Chem. B* **1999**, *103*, 6030.
31. Tamm, J.; Alumaa, A.; Hallik, A.; Johanson, U.; Tamm, L.; Tamm, T. *Russian J. Electrochem.* **2002**, *38*, 210.#